

Managing Classical Processing Requirements for Quantum Error Correction

Satvik Maurya, Swamit Tannu
University of Wisconsin-Madison

Abstract

Quantum Error Correction requires decoders to process syndromes generated by the error-correction circuits. These decoders must process syndromes faster than they are being generated to prevent a backlog of undecoded syndromes. This backlog can exponentially increase the time required to execute the program, which has resulted in the development of fast hardware decoders that accelerate decoding. Applications utilizing error-corrected quantum computers will require hundreds to thousands of logical qubits and provisioning a hardware decoder for every logical qubit can be very costly. In this work, we present a framework to reduce the number of hardware decoders and navigate the compute-performance tradeoffs without sacrificing the performance or reliability of program execution. Through workload-centric characterizations performed by our framework, we propose efficient decoder scheduling policies that can reduce the number of hardware decoders required to run a program by up to 10 \times . With the proposed framework, scalability can be achieved via decoder virtualization, and individual decoders can be built to maximize accuracy and performance.

Keywords

Virtualization, Quantum Error Correction, Decoders

1 Introduction

As quantum computing enters a phase of rapid scaling to enable Fault-Tolerant Quantum Computing (FTQC), the classical processing resources required to support Quantum Error Correcting (QEC) codes must be scaled proportionally. QEC codes generate a stream of syndromes repeatedly by measuring parity qubits every cycle, and a decoder algorithm running on the classical control computer processes the stream of syndrome bits to detect and correct errors. Recent demonstrations have shown the Surface Code [26] can be deployed experimentally to suppress logical error rates [1, 2], creating 48 logical qubits using neutral atoms [10], an 800 \times reduction in the error rate using four logical qubits [19]. These demonstrations are precursors to complex systems with more logical qubits that will require significant classical resources to enable FTQC systems.

Building a universal fault-tolerant quantum computer requires support for both Clifford and non-Clifford gates. For the Surface Code, applying a non-Clifford T -gate requires decoding prior errors so that an appropriate correction can be applied [26, 33, 39]. The decoding cannot be deferred, thus requiring decoding to be performed in real-time. Moreover, there is even a broader constraint on decoding throughput – if syndromes are generated faster than they can be processed, computation can be slowed down exponentially due to the backlog problem [57]. Qubit technologies such as superconducting qubits have fast syndrome cycle times in the order of 1 μ s [2], which require decoder latencies to be smaller than the syndrome cycle time.

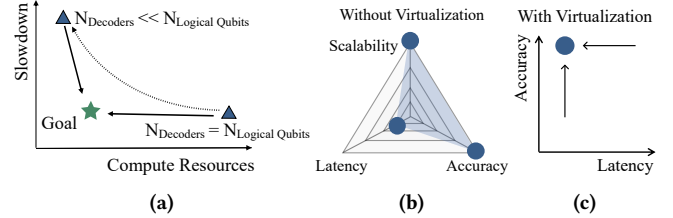


Figure 1: (a) Fewer decoders result in a slowdown in the computation due to large backlogs of undecoded syndromes. VQD avoids this slowdown in computation while reducing the number of decoders; (b) Multi-objective optimization problem for designing decoders without any virtualization – current decoders are designed to minimize latency and maximize scalability, accuracy; (c) Virtualization allows the optimization problem to be reduced to just speed and accuracy – decoder virtualization can improve scalability.

Applications that can benefit from FTQC will require hundreds to thousands of logical qubits to function [9]. Depending on the error-correcting code used, replicating decoders for *every* logical qubit in the system can become very expensive and intractable in terms of cost and complexity. This is especially because decoders add to the classical hardware already needed for qubit control and readout. To reduce this cost, fast, hardware-efficient decoders have been proposed which sacrifice some accuracy for speed and scalability [3, 5, 47, 62]. However, catering to hundreds to thousands of logical qubits with these specialized decoders will still result in complex and costly systems – in this work, we aim to show how the total number of decoders can be reduced without affecting the performance or reliability of the quantum computer, thus allowing for more scalable classical processing for QEC.

In this paper, we present **VQD: Virtual Quantum and Decoding**, a framework that aims to provide the illusion that there are decoders for every logical qubit while using significantly fewer hardware decoders to enable scalable and efficient classical processing necessary for fault-tolerant quantum computers. Reducing the number of decoders is not straightforward – if there are fewer decoders than logical qubits, some logical qubits will remain undecoded for some periods of time. When a logical qubit remains undecoded for some rounds of syndrome generation until a non-Clifford gate is executed on it, the overall decoding task is more than the original set of undecoded syndromes since syndromes keep getting generated as the decoder processes the original set of undecoded syndromes. This introduces a slowdown in the computation, as shown in Figure 1(a). The goal of this work is to avoid the slowdown in computation while reducing the compute resources required for decoding. Our experimental evaluations also show that if a logical qubit is not decoded for extended periods (which will occur if there are fewer decoders than qubits), then it can cause the decoder latency to

increase due to an increase in undecoded errors. This increase in the decoder latency can affect the application of non-Clifford states – if decoding is delayed for a logical qubit before applying a non-Clifford state, the application of the non-Clifford state could be delayed since the decoder might take more time than usual to decode all prior rounds.

Given the challenges in sharing decoder hardware and to understand how it can be enabled, we characterized representative FTQC workloads to understand the decoding requirements from a performance and reliability perspective. Our characterization using a lattice surgery compiler [63] revealed that there is a limited amount of operational parallelism due to long sequences of T and H gates resulting from Clifford + T decomposition, which is necessary for universality. This is crucial, as non-Clifford gates are the reason why real-time decoding is necessary for FTQC [57]. Non-Clifford operations are the only operations where the decoding is in the critical path, and fortunately, they occur in a highly serialized manner. Therefore, a physical decoder per logical qubit is unnecessary and will lead to severe underutilization.

Armed with this insight, we propose a system architecture with significantly fewer physical decoders than the number of logical qubits. Furthermore, we design efficient decoder scheduling policies for such systems. We propose a scheduling policy that minimizes the Longest Undecoded Sequence, termed as the MLS policy. We compare it with the Round Robin (RR) and Most Frequently Decoded (MFD) policies – our evaluations show that the MLS policy can reduce the number of hardware decoders by up to 10 \times for algorithmic logical qubits and 4 \times when magic state distillation factories are also considered, while ensuring that no logical qubit remains undecoded for a significantly long period. We show that offloading decoding tasks to software also reduce the longest period for which a logical qubit remains undecoded by up to 40%. We also propose a dynamic scheduling mechanism that can prioritize decoding for logical qubits affected by error bursts due to phenomena such as cosmic rays [42] and leakage due to heating [44].

We also analyze the effect of decoding latencies on the efficacy of virtualization. Our studies show that slow decoders are not amenable to virtualization, and QEC codes such as qLDPC codes will require significantly faster decoders than that are available today for virtualization to be possible. Through VQD, we show that the design space for decoders can be reduced from optimizing for latency, accuracy, and scalability (Figure 1(b)) to just latency and accuracy (Figure 1(c)). With VQD, we show that even if individual decoders have a high hardware cost, the overall cost can be reduced significantly by virtualizing decoders.

2 Quantum Error Correction and Decoding

In this section, we cover high-level details of Quantum Error Correction and the role of decoders.

2.1 Quantum Error Correction

Quantum Error Correction (QEC) improves the reliability of a system by utilizing many physical qubits to encode a single logical qubit [35, 50]. Most QEC codes can be categorized as stabilizer codes [57] – some promising stabilizer codes include quantum Low Distance Parity Check (qLDPC) codes [12] and Surface Codes [26].

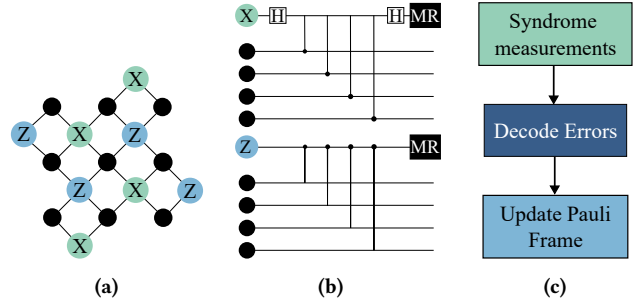


Figure 2: (a) A logical qubit ($d = 3$); (b) Syndrome generation and measurements; (c) A typical procedure for detecting errors by decoding syndromes.

Owing to their relatively relaxed connectivity requirements that can be realized with hardware available today, we focus specifically on the Surface Code.

A single rotated Surface Code patch of distance $d = 3$ is shown in Figure 2(a) [33]. Black circles denote data qubits and each data qubit is connected to X and Z parity qubits. The Surface Code works by repeatedly measuring syndromes, which correspond to the measurements performed on all X and Z measure qubits in a patch after performing the sequence of gates shown in Figure 2(b). By repeatedly measuring these syndromes, both bit-flip and phase-flip errors occurring within a patch can be detected by the decoder.

2.2 Decoding Errors

Figure 2(c) shows the general procedure of how any generic QEC code works – syndromes are constantly being generated, which are then fed to a decoder. Syndromes contain information about which qubits have flipped in every round of syndrome measurements, and these flips allow the decoder to determine what errors on the data qubits caused those flips. Since errors can always be expressed in the form of Pauli gate, they can be corrected in software without executing any physical operations on the logical qubits. This is achieved by updating the Pauli frames for all data qubits that make up that logical qubit, which adjusts the interpretation of future measurements by accounting for the error that was detected [57]. For the Surface Code, the decoding problem is commonly formulated as a Minimum Weight Perfect Matching (MWPM) problem [25, 65].

2.3 Non-Clifford Gates

On a Surface Code error-corrected quantum computer, all Clifford gates can be performed reliably either in software or via logical operations performed via Braiding [26] or Lattice Surgery [33]. However, non-Clifford gates such as the T gate cannot be applied in a fault-tolerant manner directly. This is because logical qubits initialized with the T gate will have an error probability equal to the underlying physical error rate of the system, p , thus making them impure [40]. However, multiple impure states can be used to distill fewer, purer logical qubits with a T state (known as a magic state $|m\rangle$) – this process is known as magic state distillation [13, 30].

Figure 3 shows how a T gate can be applied to a logical qubit P in a fault-tolerant manner by using Lattice Surgery (LS) [39]. The magic state $|m\rangle$ is a purified T -state. Since a non-Clifford gate is

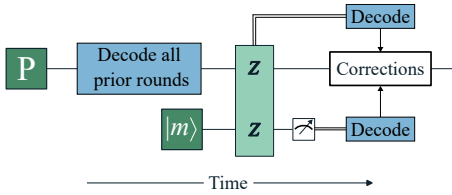


Figure 3: Consumption of a magic (T) state with LS.

being applied, all prior errors that affected P must be known before $|m\rangle$ is applied to prevent errors from spreading [57]. Lattice Surgery can be used to perform a $Z \otimes Z$ operation on P and $|m\rangle$ to apply the magic state [39, 40]. Once the $Z \otimes Z$ operation is performed, the decoding result of P prior to Lattice Surgery is combined with the decoding result of Lattice Surgery multi-body measurement and the measurement of the patch containing the magic state $|m\rangle$ to determine an appropriate Clifford correction¹. This correction needs to be known before the next logical operation involving a non-Clifford gate. **We assume the use of auto-corrected Pauli-Product Rotations (PPR) [40] for all non-Clifford gates.**

2.4 Critical Decodes

For a logical qubit that is only executing Clifford gates, errors can be decoded at any point in time (even after the experiment has ended). This is because all Clifford corrections can be commuted to the end of the circuit, essentially allowing the syndromes to be post-processed rather than decoded in real-time [57]. However, universal fault-tolerant quantum computer require non-Clifford gates such as the T -gate – this makes real-time decoding a necessity since syndromes for a patch must be decoded before the application of a non-Clifford gate. We call decodes that *must* happen before the application of a non-Clifford gate **critical decodes**, since all syndromes generated up to that point for that logical qubit must be decoded before computation can proceed. Finally, performing non-Clifford operations on logical qubits encoded in quantum Low Distance Parity Check (qLDPC) codes require a critical decode to measure the ancillary system required to transfer the logical qubit to a Surface Code patch [17].

3 Classical Processing Requirements

We now discuss the classical processing requirements for FTQC.

3.1 Syndrome Generation and Processing Rates

As discussed in Section 2, applying non-Clifford gates requires decoders to be up-to date with the latest syndrome for a logical qubit before computation can proceed. As shown by Terhal [57, p. 20], if the rate at which syndromes are generated r_{gen} is faster than the rate at which they are processed r_{proc} , the time required to execute a workload increases exponentially with the number of non-Clifford T states required by the program (the *backlog* problem [57]). Now, if every decoder in the system has an $r_{proc} > r_{gen}$, and every logical qubit has its own decoder, there will be no backlog of syndromes to be decoded and hence no slowdown in the system. Since non-Clifford operations will be very frequent in FTQC systems [8],

¹The auto-corrected $\pi/8$ gate in [39, 40] uses an additional ancillary qubit that has not been shown.

ensuring that r_{proc} is consistently greater than r_{gen} is a critical requirement for FTQC systems.

3.2 Why is Real-Time Decoding Necessary?

This requirement for syndromes to be processed faster than they are generated has motivated research to build fast and accurate hardware decoders for the Surface Code [3, 5, 47, 52, 62], especially for systems using superconducting qubit architectures due to their fast gate times. While the syndrome processing rates achieved by these decoders are far higher than typical syndrome generation rates achieved today [2, 10], leaving syndromes undecoded for many successive rounds can be problematic. Figure 4(a) shows how the decoder latency normalized to the number of rounds (latency per round) processed by the decoder can increase exponentially with the number of rounds of undecoded syndromes, especially for $d = 7, 9$ (circuit-level noise $p = 10^{-4}$). The number of rounds was chosen as a multiple of d since it represents the shortest period required for executing a logical operation [33]. This slowdown is easily explainable by the fact that errors will accumulate the longer a logical qubit remains undecoded, thus requiring more corrections to be performed. This can result in a significant slowdown, and hence a decrease in r_{proc} leading to higher memory requirements to store undecoded syndromes. However, note that the slowdown in r_{proc} will result in more rounds of error correction required to complete the computation. Figure 4(b) shows how the logical error rate grows slowly with the number of rounds for $p = 10^{-3}$, $p = 10^{-4}$ respectively. Code distances are selected to achieve a target logical error rate after the N rounds it takes to complete a program [8, 9] – critical decodes delayed exponentially due to a slow r_{proc} will exacerbate the logical error rate, since more rounds would be needed to complete the computation.

3.3 Concurrency and Delayed Decoding

Critical decodes **must** be serviced during the execution of a program to avoid the increase in memory requirements and processing times discussed above. If there are many concurrent critical decodes that occur frequently during the execution of a program, an appropriate number of decoders will be needed to process these critical decodes. The level of concurrency depends entirely on the layout used to build the quantum computer – layouts such as the Compact [39, p. 7], Fast [39, p. 9], and the Edge-Disjoint Path (EDPC) compilation [7] are some proposed layouts that can be used to build fault-tolerant quantum computers using the Surface Code. Layouts determine the number of physical qubits required – for example, the Compact layout requires the fewest physical qubits since there is a single routing lane at the cost of completely serializing operations. The Fast and EDPC layouts allow more concurrency at the cost of more physical qubits.

What is the average level of concurrency when executing a quantum program on a fault-tolerant quantum computer? Figure 4(c) shows a histogram of the number of critical decodes² for select workloads generated by the Lattice Surgery Compiler [63]. This histogram shows that the peak concurrency is attained very infrequently. This implies that most logical qubits function as memory

²For the Surface Code, we assume every logical qubit requires two decoders – one each for the X and Z observables.

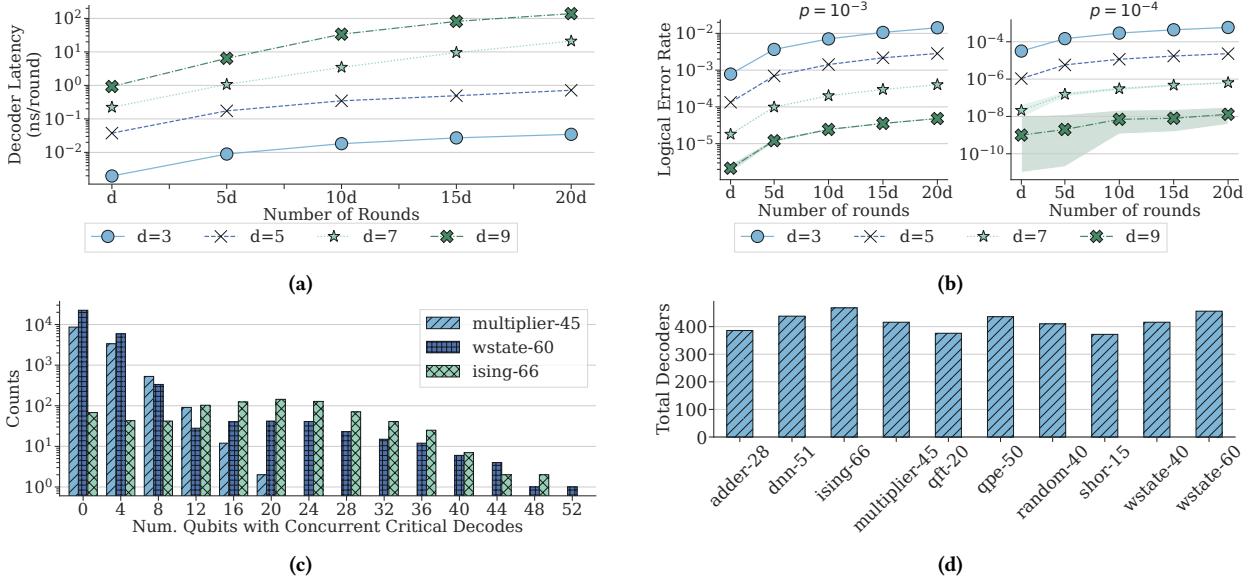


Figure 4: (a) Exponential increase in the decoder latency per round (in nanoseconds) as the number of rounds is increased from d to $20d$ – the increase is higher for larger code distances ($p = 10^{-4}$); (b) Slow increase in the logical error rate as the number of rounds of error correction increase with $p = 10^{-3}$, $p = 10^{-4}$; (c) Histogram of the number of concurrent critical decodes for different workloads with the EDC layout – there is limited parallelism as far as critical decodes are concerned; (d) Estimated total decoders required for different workloads with the EDC layout and 24 distillation factories for every workload.

qubits or execute Clifford gates more often than T -gates, and this can allow some qubits to not be decoded in real-time.

Quantum programs are serial in terms of T -gates applied – not every qubit requires constant access to a fast decoder.

3.4 Goal: Make Classical Processing Efficient

Provisioning a hardware decoder for every logical qubit in the system can be resource intensive. Figure 4(d) shows an estimate of the total number of decoders required for all logical qubits (=algorithmic, ancillary, magic state storage, and magic state distillation logical qubits) when using the EDC layout for different workloads. These estimates were obtained by using Lattice Surgery Compiler [36, 63]. Note that the total hardware requirement will be significantly higher because of control and readout components. Having shown how the syndrome processing rate is crucial in ensuring that computation does not require excessive memory and time and how quantum programs are inherently serial in terms of critical decodes, the question we seek to answer in this work is –

How can we minimize the use of hardware decoders and lower classical processing costs without sacrificing performance and reliability?

4 VQD: Virtual Quantum Decoding

We now discuss decoder virtualization, where there are fewer hardware decoders than logical qubits in the system, and how decoding can be scheduled optimally.

4.1 Working with Fewer Hardware Decoders

Reducing the number of available decoders implies that qubits will share hardware resources, resulting in time-division multiplexing of decoder instances among logical qubits. Figure 5 shows how compared to a system with decoders for every logical qubit in the system (N qubits, N decoders), a system with fewer (M , $N > M$) decoders will require resources to be shared with time.

Time-division multiplexing of hardware resources will require the following considerations: (i) If the number of critical decodes at a given time step exceed the number of hardware decoders, the overflowing critical decodes will have to be deferred to the next available time step, and (ii) Qubits cannot be left undecoded for extended periods of time. For the first consideration, deferring critical decodes will increase serialization in the program – this offsets all benefits offered by the Fast and EDC layouts. For the second consideration, leaving a qubit undecoded for too long will result in an exponential increase in the syndrome processing latency and memory required to store undecoded syndromes.

Since not all qubits will be involved in critical decodes at every time step, there will be some decoders available at a given point of time which will not be decoding a logical qubit involved in the consumption of a T -state. Allocating these *free* hardware decoders to logical qubits at every time thus becomes a scheduling problem.

Before we discuss different decoder scheduling policies, it is important to understand the time granularity at which any scheduling policy will operate on. Since logical operations (Clifford or non-Clifford) in a Surface Code error-corrected quantum computer will require at least d rounds before the next operations, we define a *slice* [63] as the smallest time step between logical operations that a decoder scheduling policy can work on. Every slice consists of d

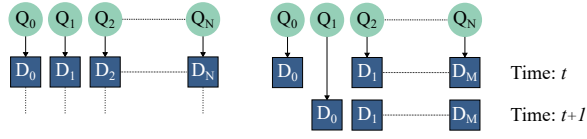


Figure 5: (Left) Decoders for every logical qubit; (Right) Time-division multiplexing of decoders between qubits.

rounds of syndrome measurements, thus making the scheduling policy agnostic of the actual code distance used.

4.2 Decoder Scheduling Policies

Static decoder scheduling refers to decoder scheduling that can be performed at compile time. Since most quantum programs do not have any control-flow instructions, scheduling can be performed statically. Scheduling decoders is similar to CPU scheduling performed by all operating systems today, where the number of processes is more than the number of available processor cores [41]. **Longest Undecoded Sequence:** To quantify the fairness of a decoder scheduling policy, we use ‘Longest Undecoded Sequence’, which measures how well the decoders are servicing all logical qubits. A large undecoded sequence length implies that a qubit has been left undecoded for a long time – increasing the memory consumed to store undecoded syndromes. Figure 6(a) shows an example of determining the longest undecoded sequence length.

Consider an arbitrary time slice t in the execution of a quantum program. There are N logical qubits and M hardware decoders ($N > M$). All decoding scheduling policies will have two components: The first will assign the decoders necessary for all critical decodes C in the time slice t . The second will assign all the remaining $M - C$ hardware decoders to the $N - C$ qubits based on the scheduling policy used. We now discuss three decoder scheduling policies (all policies are illustrated in Figure 6(b) – Figure 6(d)):

4.2.1 Most Frequently Critically Decoded (MFD). A logical qubit that consumes a significant number of T -states during the execution of a program would have a frequent requirement of critical decodes – leaving such a logical qubit undecoded for more than a few slices would make subsequent critical decodes take longer, thus slowing down computation. This motivates the MFD scheduling policy that prioritizes decoding of logical qubits that have numerous critical decodes in the future at any given time slice (Figure 6(b)). The MFD policy will ensure that future critical decodes have a minimized number of undecoded syndromes for the qubits that have frequent critical decodes.

Caveats: Because the MFD policy prioritizes logical qubits with frequent critical decodes, it will likely starve other qubits of decoding, leading to longer undecoded sequences.

4.2.2 Round Robin (RR). Derived from CPU scheduling policies used by operating systems, the RR policy does not prioritize any specific logical qubits – rather, it chooses $M - C$ qubits in a round-robin manner (Figure 6(c)) in every time slice to ensure fairness for all qubits in the system.

Caveats: For regions of a program where there are many critical decodes, the RR policy could still starve some logical qubits since $M - C$ will be much smaller, yielding a smaller window for decoders to be assigned. Since there is no prioritization, the RR policy will

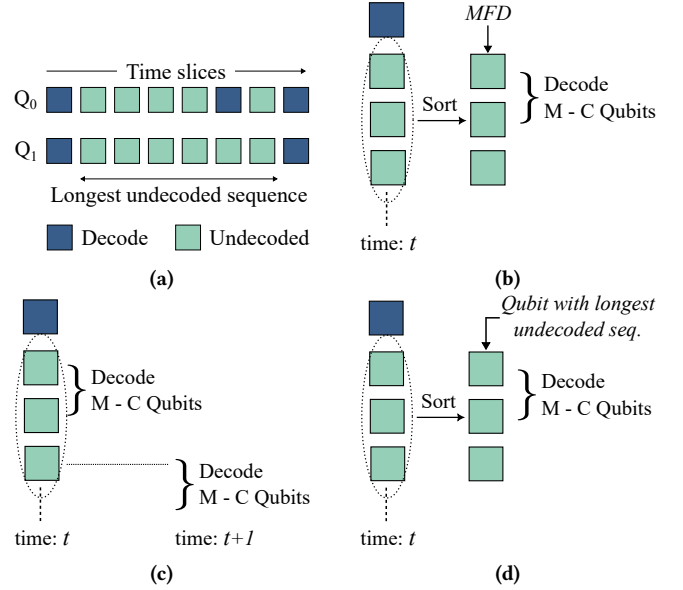


Figure 6: (a) Illustration of the longest undecoded sequence – Q_1 has the longest undecoded sequence before the last decode; (b) MFD policy – undecoded qubits are sorted according to the number of critical decodes they are involved in after time slice t and $M - C$ qubits are selected from this sorted list; (c) RR policy – the $M - C$ qubits decoded in time slice t are not decoded in time slice $t + 1$; (d) MLS policy – undecoded qubits are sorted according to their undecoded sequence lengths and $M - C$ qubits are selected from this sorted list.

not be able to rectify this until the round-robin window reaches the qubits being starved.

4.2.3 Minimize Longest Undecoded Sequence (MLS). The longest undecoded sequence length at any given time slice is an indicator of how well the decoder scheduling policy is servicing all qubits in the system. We use this as a motivator for the MLS policy, which tries to minimize the longest undecoded sequence at every time slice (Figure 6(d)). The MLS policy works as follows: at any time slice t , qubits are sorted on the basis of their current undecoded sequence lengths. Then, $M - C$ qubits with the largest undecoded sequence lengths are assigned hardware decoders.

Caveats: In cases where there the number of logical qubits is far greater than the number of decoders ($N \gg M$), the MLS policy will not be able to work effectively.

4.3 Noise-Adaptive Decoder Scheduling

While control-flow instructions would necessitate runtime scheduling of decoders, events such as cosmic rays [42] and leakage [44] can result in a temporary burst of errors for some physical qubits in the lattice that can impact some logical qubits. Detecting a spike in the physical error rate will either require errors to be decoded or additional hardware modules to detect the spike. As shown in Figure 7(a), an increase in the physical error rate results in a higher number of bit-flips (especially for larger code distances), which can be detected with simple components in the control hardware.

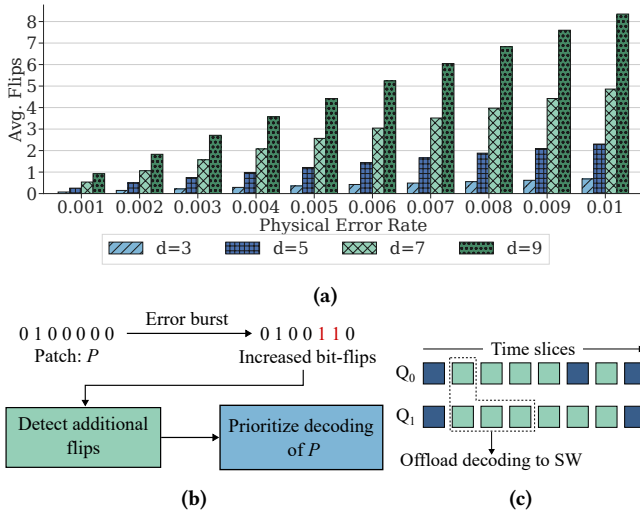


Figure 7: (a) Increase in the average number of bit-flips in syndromes for different code distances as the physical error rate is increased; (b) An error burst results in increased bit-flips in the syndromes of patch P which can be detected and used to prioritize the decoding of P in the next time step; (c) Decoding can be offloaded to software provided there is enough time before a critical decode occurs.

Figure 7(b) shows how additional flips can be detected and used to dynamically prioritize the decoding of an arbitrary patch P , which suffers from a temporary burst of errors. Note that the detection is different from decoding – we are merely predicting that there are more errors due to higher bit-flips in the syndromes. Unlike prior work [55], this mechanism only prioritizes the decoding of logical qubits affected by error bursts in a virtualized decoder environment. However, this prioritization can result in reduced efficacy of virtualization, due to fewer decoders being available for scheduling during error burst events. We evaluate the overheads of such error bursts for virtualization in Section 7.

4.4 Offloading to Software Decoders

Software decoders are slow and also have a higher variance in decoding latencies [23]. However, when scheduling decoding tasks for logical qubits, software decoders can be leveraged to further reduce the undecoded sequence lengths. As shown in Figure 7(c), some syndromes for a logical qubit can be offloaded to software while the hardware decoders are busy elsewhere. To prevent scheduled hardware decoding from being delayed, a buffer (three slices in this example) must be used to ensure that the software offloading completes before the next hardware decode.

4.5 Decoding for Distillation Factories

The decoder scheduling policies in the previous sections catered only to the decoding of algorithmic logical qubits (data logical qubits, magic state storage, ancillary logical qubits required for Lattice Surgery). Magic state distillation factories generate few lower error logical qubits with non-Clifford states from many high-error logical qubits. Distillation factories run for very short periods at a

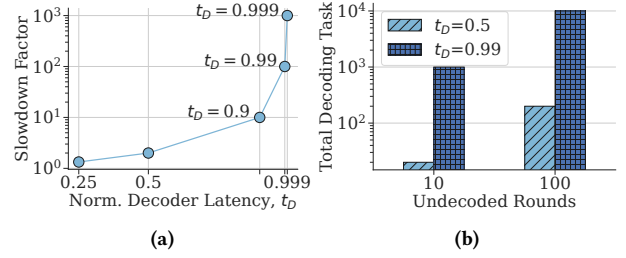


Figure 8: (a) Slowdown in the processing of outstanding syndromes for different normalized decoder latencies $t_D = T_{proc}/T_{gen}$. Slower decoders require more time (and thus more rounds) to catch up with the present syndrome; (b) Differences in the total decoding task for different initial undecoded rounds – a $t_D = 0.99$ increases the number of rounds to be decoded by a 100 \times .

time – this allows for smaller code distances to be used for creating the logical qubits for distillation [40]. Smaller code distances for distillation factories provide two main benefits: the number of physical qubits required are much lower, and more importantly, both hardware [16, 22, 52, 62] and software [23] decoders are faster and less complex. For example, LUT based decoders [20] have been shown to be effective up to $d = 5$ without requiring significant hardware resources. Predecoders [22, 47, 52] reduce the complexity and decoding effort required for lower code distances as well. Compared to algorithmic logical qubits, which require a large code distance to survive millions of error correction cycles [8, 9], the decoding requirements of distillation factories are far more relaxed, which reduces the hardware resource requirements as well.

Magic state distillation has lower hardware requirements for decoding due to lower code distances involved – and virtualization can further reduce them.

4.6 Impact of Decoding Latencies

So far, we have considered decoder virtualization without considering the decoder latency. However, the former is heavily impacted by the latter. Consider a scenario where a logical qubit has R undecoded rounds prior to a critical/scheduled decode. Now, the decoder will take a finite time to process these R rounds worth of syndromes based on its per round decoding latency T_{proc} . However, during the time the initial R rounds of syndromes are processed, syndromes are continuously generated based on the syndrome generation time T_{gen} . Thus, at any time t , the total rounds processed are $P(t) = t/T_{proc}$, the syndrome rounds generated are $G(t) = t/T_{gen}$, and so, the outstanding rounds to be processed can be defined as $S(t) = R + G(t) - P(t)$. The total time taken for the decoder to catch up is thus t_{total} , with $S(t_{total}) = 0$, and hence:

$$t_{total} = \frac{R}{T_{proc}^{-1} - T_{gen}^{-1}}; \text{ (iff } T_{proc} < T_{gen} \text{)} \quad (1)$$

T_{proc} has a considerable effect on the efficacy of decoder virtualization, since a slower processing rate would mean that a huge number of additional rounds will be required for the decoder to be able to catch up to the present syndrome being generated. This can

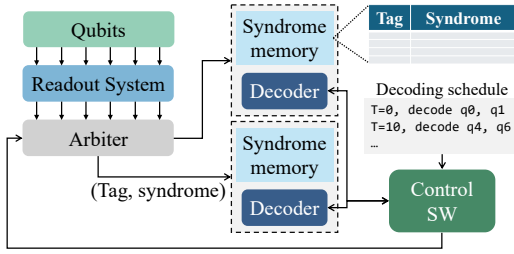


Figure 9: System architecture for virtualized decoding.

be seen from Figure 8(a), where the decoder latency is normalized by the syndrome generation time $t_D = T_{proc}/T_{gen}$ and the slowdown is defined as the ratio of the total time taken to process R undecoded rounds (Equation 1) and the ideal time when extra syndromes are added to the decoding task ($t'_{total} = R/T_{proc}$, $slowdown = t_{total}/t'_{total}$). This slowdown is agnostic of the actual implementation of the decoder – techniques like parallel window decoding [51] will only help reduce the value of t_D . Figure 8(a) shows the **total decoding task** ($P(t_{total})$), which represents the total syndromes that need to be processed for an initial R undecoded rounds. From Figure 8(a), we see that the closer the decoding processing rate is to the syndrome generation rate ($t_D = 0.99$), the harder virtualization will be, since even $R = 10$ will require 10^4 rounds before the decoder can catch up. **This is a crucial limitation for decoder virtualization, and it also suggests that faster, more accurate decoders will be more desirable than fast decoders which have a smaller hardware footprint at the cost of accuracy.** Figure 8(b) shows an example for cases where there are 10/100 undecoded rounds before the decoder is invoked for a logical qubit – a slower decoder will require thousands of extra rounds to catch up compared to a faster decoder! Running so many additional rounds will slow down the system, reduce the error budget per round of computation, exacerbating the logical error rates. In Section 7, we will show how slow decoders associated with qLPDC codes are not amenable for virtualization, due to the slowdown they incur for even modest undecoded sequence lengths. This represents a limit of virtualization, and motivates further research in developing fast, accurate decoders for all QEC codes.

5 System Architecture with Virtual Decoders

Enabling the virtualization of decoders in an FTQC system requires (i) memory to store syndromes of logical qubits that are not being decoded at any time, and (ii) a mechanism for selecting the qubits to be decoded by a specific decoder at any time. Figure 9 shows the system architecture that can be used for enabled virtualized decoders. The Arbiter is a key component that routes syndromes from the readout system to the decoders. Since there will be fewer decoders than logical qubits, syndromes will be routed based on the static decoding schedule prepared during compile time. To allow decoders to access the syndromes of a specific logical qubit at any given point in time, the arbiter attaches a tag to the syndromes before routing them to the appropriate decoder. This tag quickly identifies the logical qubit to which a syndrome belongs to. Every decoder consists of a syndrome memory, and the decoding schedule

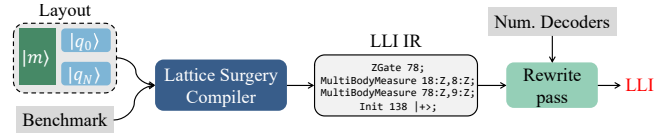


Figure 10: Compilation framework – the rewrite pass changes the IR schedule based on the number of available decoders.

can be used by the control software to access the syndromes of any logical qubit from the syndrome memory.

Software offloading can be easily integrated in the design by enabling the syndrome memory to be read from the control software. Note that this will require high-speed links between the control software and the decoder modules, such as the low-latency ethernet used in recent experimental demonstrations [1]. The control software can specify the tag and the syndromes to be read from the syndrome memory. This will however require fusing the software decoding results with the hardware decoding results. Fusion of separate decoding tasks has also been demonstrated recently by Google [1]. To enable dynamic decoder scheduling, the control software need only trigger decoding for the necessary logical qubit(s) by amending the decoding schedule. Since this could trigger the decoding of any arbitrary logical qubit, the syndrome memories must support random accesses. No other changes to the Arbiter are necessary, since syndromes can be routed to the same memory regardless of dynamic scheduling that could occur later in time.

6 Methodology

We now describe the methodology used to evaluate different decoder scheduling policies and classical processing requirements.

6.1 Compiler

We use the Lattice Surgery Compiler (LSC) [63] to generate Lattice Surgery Instructions (LLI) Intermediate Representations (IR) of workloads that can be executed on an error-corrected quantum computer using the Surface Code with lattice Surgery. LSC can generate IR that denote Lattice Surgery instructions from the QASM [18] representation of a workload. The Lattice Surgery instructions generated by LSC are a combination of Clifford operations and multi-body measurements used for implementing Pauli-Product Rotations (PPR) [39]. LSC handles mapping and routing based on the layout provided to the compiler, as shown in Figure 10. We configure LSC to use a ‘wave’ scheduling that maximizes the number of concurrent instructions executed in every time slice. LSC uses Gridsynth [49] to deal with arbitrary rotations. However, since it is still under development, LSC has some limitations:

- LSC is limited to multi-body measurements between only two logical qubits.
- LSC treats distillation factories as black boxes.
- LSC works for a limited set of layouts and is extremely slow for large workloads like shor.

6.2 Simulation Framework

Using the IR generated by LSC, we build a framework³ that can parse the IR and determine the critical decodes in every slice, generate a timeline of all operations, and assign decoders to all logical qubits depending on the scheduling policy. In case the number of critical decodes in a particular slice are more than the number of hardware decoders configured, decoder-resources can rewrite the IR to defer critical decodes to the next slice.

Layouts: We use three layouts for our evaluations – Fast, Compact [39], and the EDPC [7] layouts. The Compact layout uses the fewest logical qubits and, due to a single routing lane, allows only one magic state to be consumed per time slice – we thus use it only to compare total execution times with the Fast and EDPC layouts.

Benchmarks: We use benchmarks from [46] and [37]. We use *shor-15*, phase estimation *qpe-50*, Quantum Fourier Transform *qft-20*, arithmetic workloads *adder-28*, *multiplier-45*. We also use a neural network workload *dnn-51*, W state workloads *wstate-40/60*, random unitary *random-40*, and an Ising model *ising-66*.

Other Software: Stim [28] was used for simulating stabilizer circuits to generate syndromes and error rates. Azure QRE [8] was used for resource estimations.

7 Evaluations

In this section, we present some results for different scheduling policies and savings in decoder hardware.

7.1 Research Questions

We aim to answer the following questions:

- (1) How many decoders can we virtualize in the system without affecting performance?
- (2) How long do qubits go undecoded when using virtualization?
- (3) How does virtualization affect Magic State Distillation?
- (4) How do error bursts affect decoder resource requirements?
- (5) How do slow decoders for qLDPC codes affect the efficacy of virtualization?

7.2 Baseline Statistics

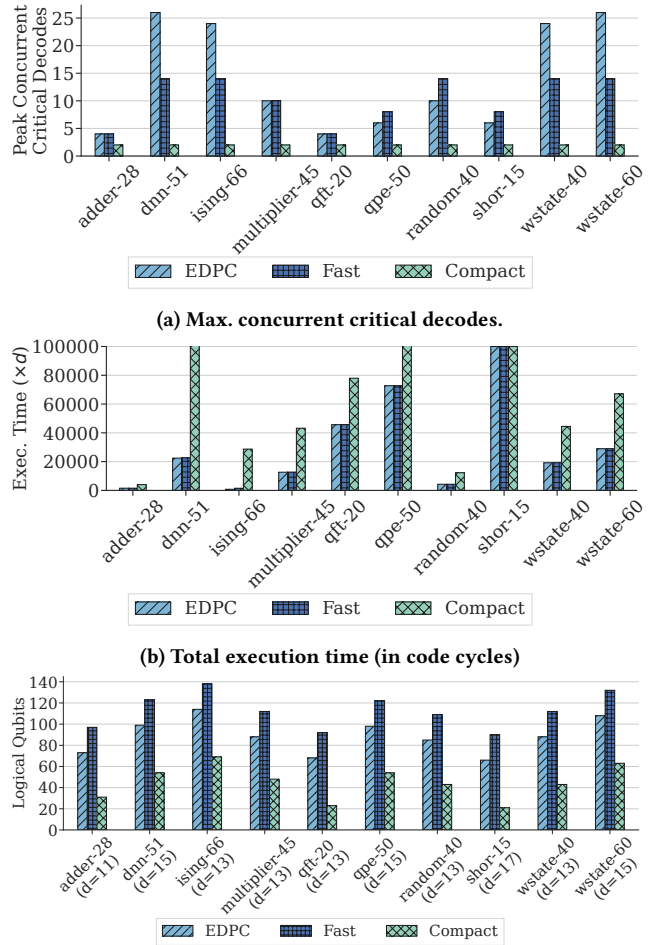
We consider the baseline to have decoders for every logical qubit in the system. Figure 11(a) shows the maximum number of critical decodes that occur during the execution of different workloads for all selected layouts. The Compact layout has a maximum of one critical decode per slice between two logical qubits. Figure 11(b) shows the total time required to finish all workloads⁴ – the EDPC and Fast layouts are significantly faster than Compact, and the EDPC layout has a very slight advantage over Fast for most workloads and also uses fewer qubits 11(c) (only algorithmic logical qubits). Due to its higher degree of parallelism (due to its better use of routing lanes), we only consider the EDPC layout for all further evaluations.

7.3 Decoder Scheduling Efficacy

Figure 12 shows the three decoder configurations used in this work.

³<https://anonymous.4open.science/r/decoder-resources-5EC4/>

⁴*shor-15* and *qpe-50* were stopped prematurely due to long runtimes (*shor-15* after 100,000 time slices for all layouts, *qpe-50* after 72,000 time slices for Fast, EDPC, and 100,000 time slices for Compact).



(c) Estimated number of logical qubits (code distances estimated by Azure QRE [8] also annotated).

Figure 11: Baseline statistics.

- The **All Qubits** configuration denotes the baseline where all qubits have a decoder.
- **Max. Concurrency** is the configuration where the number of hardware decoders in the system corresponds to the peak concurrent critical decodes for every workload shown in Figure 11(a).
- **Midpoint** refers to a configuration where the number of hardware decoders is the midpoint between the max. and min. concurrent critical decodes ($= \frac{Max.+Min.}{2}$).

The minimum concurrent critical decodes corresponds to one critical decode between two logical qubits because a multi-body measurement merges the two patches into a single decoding task. We first focus our evaluations on **algorithmic** logical qubits, and then incorporate distillation factories as well. For the **All Qubits** configuration, the longest undecoded sequence length will be zero, since every logical qubit has an assigned decoder.

7.3.1 Longest Undecoded Sequences. To evaluate the performance of the decoder scheduling policies described in Section 4, we determine the longest undecoded sequence lengths for all workloads

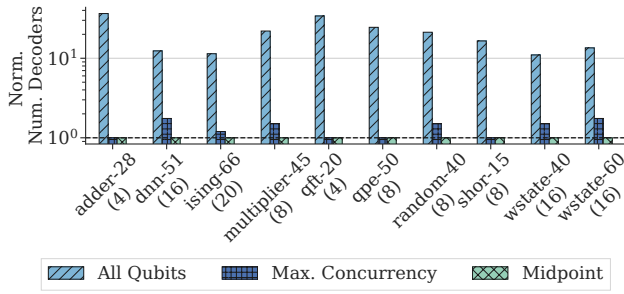


Figure 12: Hardware decoders normalized with the Midpoint configuration (EDPC layout). Decoders used by the Midpoint configuration are annotated below the benchmarks.

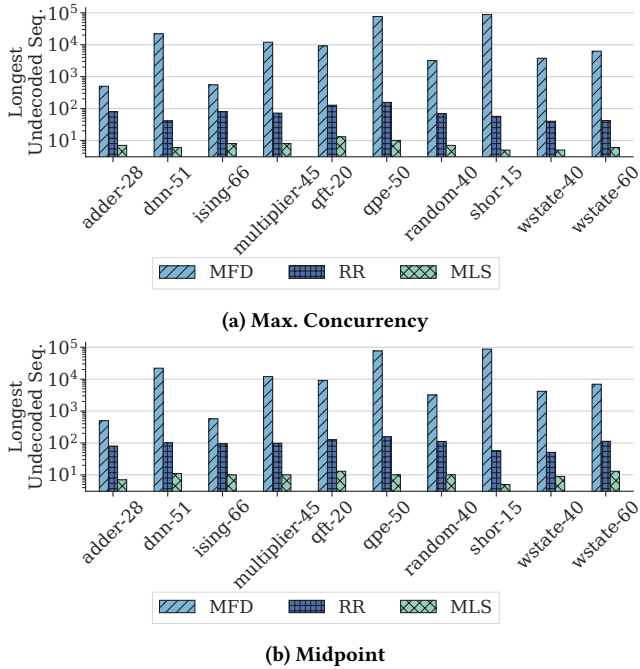


Figure 13: Longest undecoded sequence when using the (a) Max. Concurrence; (b) Midpoint configurations.

when using the **Max. Concurrence** and **Midpoint** configurations. Since these configurations use far fewer hardware decoders than qubits, the longest undecoded sequence is a good measure of whether qubits are being starved of decoding. Figure 13 shows the longest undecoded sequence lengths for the (a) **Max. Concurrence** and (b) **Midpoint** configurations. The MFD policy leads to qubits being starved of decoding, since it prioritizes qubits that have frequent critical decodes. While the RR policy performs significantly better than the MFD policy, the MLS policy consistently performs better than both policies – MLS reduces the longest undecoded sequence lengths for almost every workload to ~ 10 time slices for both **Max. Concurrence** and **Midpoint** configurations.

7.3.2 Memory Usage. The reduction in the longest undecoded sequence lengths also corresponds to lower memory usage for storing undecoded syndromes. Figure 14 shows the memory required for

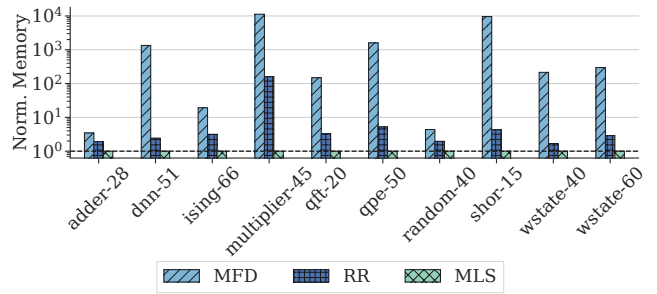


Figure 14: Memory required (normalized by the MLS policy) for undecoded syndromes with the Midpoint configuration.

different workloads with the **Midpoint** configuration (memory requirements were determined using the code distances estimated by Azure QRE). Due to longer undecoded sequences, the MFD policy can require 3–4 orders of magnitude more memory than the MLS policy, which requires around 0.01MB of memory. The RR policy can require 3–10 \times more memory than the MLS policy.

7.3.3 Software Offloading. The longest undecoded sequences can be reduced further by leveraging software decoders. The only constraint while doing so is that critical decodes should not be delayed because prior software decodes for a logical qubit have not yet finished. For evaluating the effect of software decoding, we set the number of hardware decoders to the **Midpoint** configuration and make a pessimistic assumption that a single slice worth of syndromes takes three time slices (about $3 \times d$ microseconds) to be decoded in software (in reality, it could be much lower with optimized software decoders [31]). Figure 15 shows the reduction in the longest undecoded sequence length for all scheduling policies when software offloading is performed – software offloading can achieve a reduction of more than 30%.

7.3.4 Incorporating Magic State Distillation. So far, our evaluations have considered only algorithmic logical qubits. Since Lattice Surgery Compiler takes the qubit layout as an input, we fixed the number and locations of magic state distillation (MSD) factories in the EDPC layout at 24 for all workloads. This number was chosen to maintain a uniform EDPC layout across all workloads, and it is also the median number of MSD factories estimated by Azure QRE (annotated below the benchmarks names in Figure 16). 15-to-1

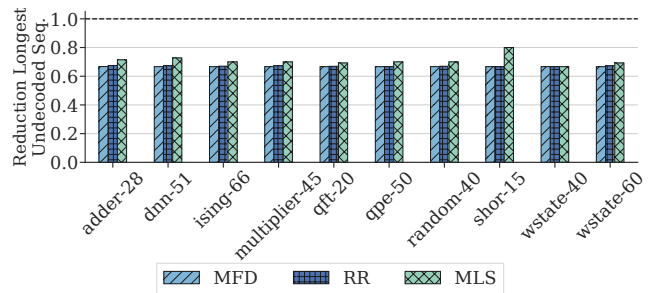


Figure 15: Reduction in the longest undecoded sequence length when using the Midpoint configuration with software offloading.

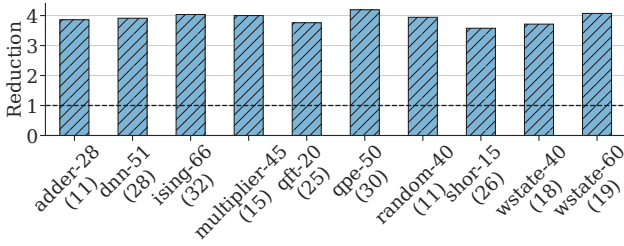


Figure 16: Total reduction in decoders required when considering 15-to-1 MSD factories with the Midpoint configuration, EDP layout. The number of MSD factories was fixed at 24 for all workloads, and the number of factories estimated by Azure QRE are annotated below the benchmark names.

distillation is mapped to a Compact layout [39]. Using this layout and the QASM circuit for a 15-to-1 MSD factory, the MLS policy was used to virtualize decoders. Table 1 shows the reduction in the number of decoders and the longest period for which a qubit remains undecoded for a single distillation factory. A 15-to-1 distillation factory requires five logical qubits [39] and with two decoders each for X/Z observables if all qubits are supplied their own decoders. This can be reduced by 60% to 4 decoders with virtualization.

Table 1: Virtualizing decoders using the MLS policy can reduce the decoders required for 15-to-1 distillation without a substantial backlog of undecoded slices.

	All Qubits	After Virtualization	Longest Undecoded Sequence Length
15-to-1 Distillation	10 decoders	4 decoders	4 time slices

Assuming that decoders are independent for every MSD factory, the reduction in the number of decoders can be computed using data from Figure 12 and Table 1, as shown in Figure 16. The MLS policy can reduce the total number of decoders required by up to 4 \times . MSD is a probabilistic process, and factories will not be in sync. at all times. Thus, treating decoders for all factories to be independent is a conservative setting – in reality, it is likely that decoders can be virtualized *among* multiple factories, which can yield further reductions in the number of decoders in the system.

7.3.5 Dynamic Scheduling. Periodic events such as heating effects, cosmic rays, can result in a temporary increase in the error rate for some qubits. Such error bursts can necessitate dynamic scheduling of decoding for affected qubits. For evaluating the overheads of such error bursts on the virtualized decoders, we configured a burst probability P_{Burst} . For a workload requiring N slices, $P_{Burst} \times N$ slices are randomly selected from which an active logical qubit is selected with a probability of P_{Burst} to be decoded. Figure 17 shows the increase in the decoders required for different P_{Burst} – dynamic scheduling only increases the decoder resource requirements for a 10% probability of a burst error happening. This shows that virtualization is effective even with moderate error burst probabilities.

7.3.6 Slowdown due to Decoding Latencies. Do slow and complex decoders, such as the ones used for qLDPC codes, work well with

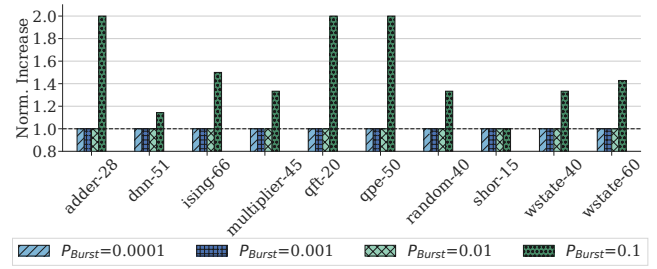


Figure 17: Normalized increase in the number of decoders required with the Midpoint configuration due to error bursts with probability P_{Burst} .

virtualization? Processing undecoded syndromes requires an additional number of rounds that is dependent on the decoding processing rate. For the Surface Code (SC), decoders that process syndromes significantly faster than the syndrome generation rate have been proposed [5, 62, 66]. However, unlike the Surface Code, quantum LDPC codes [12, 29, 32, 48, 64] have considerably slower decoders with software latencies in the order of milliseconds. To put that in context, software decoders for the Surface Code have microsecond latencies [31]. Assuming accelerated decoders for qLDPC codes are designed, it is reasonable to expect them to be slower than Surface Code decoders. To see the impact of such slow decoders on virtualization, we modified our framework to support heterogeneous systems consisting of qLDPC blocks and Surface Code patches for compute [54]. To do this, we assumed every magic state

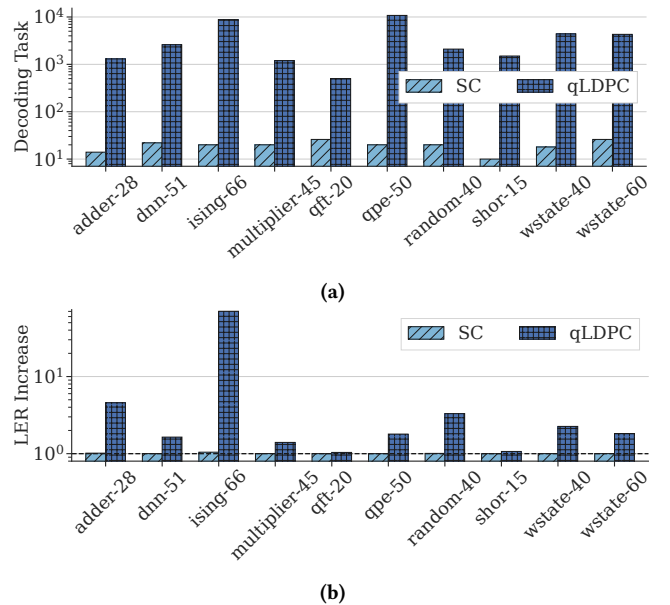


Figure 18: (a) Total decoding task required to process the longest undecoded sequence of syndromes for all workloads, with the normalized decoder latency for the Surface Code (SC) as 0.5 and 0.99 for the qLDPC code. The Midpoint configuration was used for both cases; (b) Relative increase in the LER for different workloads for the SC and qLDPC setups.

consumed involved an additional decoder to decode the ancillary system required for computation with qLDPC codes [17].

In previous sections, we have shown how the MLS policy with the **Midpoint** configuration reduces the longest undecoded sequence length to ~ 10 time slices for the Surface Code. We repeat virtualization with the Surface + qLDPC code system to determine the longest undecoded sequence. Figure 18(a) shows the total decoding task needed to decode the longest undecoded sequence for all workloads. The normalized decoding latency ($t_D = T_{proc}/T_{gen}$) was set as 0.5 and 0.99 for the Surface and qLDPC codes, respectively. Figure 18(b) shows the increase in the logical error rate (LER) due to the extra slices needed to process the undecoded syndromes – the small number of slices required for the SC results in a miniscule increase in the LER, whereas the qLDPC + Surface Code system incurs a significant LER penalty $> \sim 2\times$. This estimate in the increase in LER was performed by assuming a final LER of 10^{-9} and determining the per slice LER by dividing the final LER with the total number of slices for all workloads. With the **Midpoint** configuration, *ising-66* incurs a longest undecoded sequence length of 88 (between two ancillary system decodes), due to its short circuit depth, parallel nature (Figure 4(c)), and additional decoders required by the qLDPC ancillary system. This increases the LER by $60\times$.

The results above show that the benefits of virtualization are only apparent when the decoding latency is much smaller than the syndrome generation latency. For both qLDPC and Surface Codes, it is thus highly desirable to have short decoding latencies, since this can enable more efficient virtualization. **Decoders thus need not be designed for resource efficiency – they can be built for speed and accuracy. Resource savings can be attained at a system-level via virtualization.**

7.4 Discussion

The results shown in previous sections show that VQD reduces the number of hardware decoders for algorithmic logical qubits by nearly one order of magnitude for most workloads with the **Midpoint** configuration, which, when combined with the MLS scheduling policy, results in significantly small undecoded sequence lengths of ~ 10 time slices. With the inclusion of distillation factories, the total reduction in the number of decoders is up to $4\times$.

Faster or Resource Efficient Decoders?: The faster a decoder is in relation to the syndrome generation latency, the more effective is decoder virtualization. Decoders with smaller hardware footprints [5, 62] generally sacrifice decoding accuracy for speed and hardware-efficiency. This work indicates that hardware-efficiency can be achieved with effective decoder virtualization on a system-level rather than at a module-level by leveraging fast, accurate decoders that need not be hardware efficient by themselves. This lends more motivation to the design of neural network decoders [1, 6], which can be resource intensive but offer code distance independent decoding latencies and can leverage existing hardware (CPUs/GPUs) rather than require custom FPGA/ASIC solutions. This insight can be applied to build fast and accurate decoders for other codes such as qLDPC, Color codes as well.

Better Capacity Planning: We envision large-scale quantum computers will be closely integrated with HPC-style systems, where scientific applications can leverage quantum subroutines using

QPUs [14]. In this setting, non-critical software decoders can run on traditional HPC platforms to alleviate the pressure on hardware decoders. Moreover, the virtualization of decoders can help us harness shot-level parallelism – all quantum programs, even on FTQC, must be executed multiple times. We can concurrently run the copies of quantum programs on multiple QPUs. However, quantum resources increase linearly for running “ k ” copies concurrently. Our work, VQD, shows that with decoder virtualization, we can enable effective sharing of classical resources, dramatically reducing overall costs and improving resource utilization.

8 Related Work

This is one of the first works to perform a workload-oriented study of the classical processing requirements and system-level scheduling policies for error-corrected quantum computers. Prior to this work, Bombin et al. [11] introduced modular decoding, which is the closest work that divides the global decoding task to sub-tasks without sacrificing decoder accuracy. However, this work, and other works such as parallelized window decoding [51, 56] always assume decoders for every logical qubit. This work shows that not all qubits require access to fast decoders at all times, thus allowing decoders to be virtualized. Other works that are broadly connected to this work are summarized below.

System-level Studies: Delfosse et al. [23] studied the speed vs. accuracy tradeoff for decoders used in FTQC. XQSim [15] is a full-system FTQC simulator. Stein et al. [53] proposed a heterogeneous architecture for FTQC, virtual logical qubits were proposed in [4], Lin et al. [38] explored modular architectures for error-correcting codes and scheduling for distillation factories was proposed in [24]. [34] described a blueprint of a fault-tolerant quantum computer.

Decoder Designs: Neural network based decoders [1, 6, 27, 43, 45, 60, 61], LUT-based decoders [20, 58], decoders based on the union-find algorithm [5, 21, 66], and optimized MWPM decoders [3, 62] have been proposed. In general, neural network decoders are generally far slower and therefore not ideal for fast qubit technologies such as superconducting qubits. Other predecoders [22, 52] and partial decoders [16] have also been proposed. Decoders based on superconducting logic [47, 59] target cryogenic implementations.

9 Conclusions

Scaling quantum computers to enable Quantum Error Correction will require specialized hardware for decoding errors. Prior work has focused on reducing the hardware resources required to build decoders. In this work, we take a full-system view and show that with the right decoder scheduling policy, it is not necessary for an error-corrected quantum computer to provide every logical qubit with a dedicated hardware decoder. The MLS policy enables the reduction of hardware decoders by up to $10\times$ without increasing the program execution time or the target logical error rate. The efficacy of the MLS policy is enhanced with software offloading of some decoding tasks. We also propose a noise-adaptive scheduling mechanism that can prioritize the decoding of logical qubits that incur a temporary increase in the physical error rate. Via virtualization, decoder systems can be made more scalable, and this insight can allow algorithm and hardware designers to focus on making decoders faster and more accurate, no matter the hardware cost.

References

- [1] Rajeev Acharya, Laleh Aghababae-Beni, Igor Aleiner, Trond I. Andersen, Markus Ansmann, Frank Arute, Kunal Arya, Abraham Asfaw, Nikita Astrakhantsev, Juan Atalaya, Ryan Babbush, Dave Bacon, Brian Ballard, Joseph C. Bardin, Johannes Bausch, Andreas Bengtsson, Alexander Bilmes, Sam Blackwell, Sergio Boixo, Gina Bortoli, Alexandre Bourassa, Jenna Bovaird, Leon Brill, Michael Broughton, David A. Browne, Brett Buckley, Bob B. Buckley, David A. Buell, Tim Burger, Brian Burkett, Nicholas Bushnell, Anthony Cabrera, Juan Campero, Hung-Shen Chang, Yu Chen, Zijun Chen, Ben Chiaro, Desmond Chik, Charina Chou, Jahan Claes, Agnetta Y. Cleland, Josh Cogan, Roberto Collins, Paul Conner, William Courtney, Alexander L. Crook, Ben Curtin, Sayan Das, Alex Davies, Laura De Lorenzo, Dripto M. Debroy, Sean Demura, Michel Devoret, Agustin Di Paolo, Paul Donohoe, Ilya Drozdov, Andrew Dunsworth, Clint Earle, Thomas Edlich, Alec Eickbusch, Aviv Moshe Elbag, Mahmoud Elzouka, Catherine Erickson, Lara Faoro, Edward Farhi, Vinicius S. Ferreira, Leslie Flores Burgos, Ebrahim Forati, Austin G. Fowler, Brooks Foxen, Suhas Ganjam, Gonzalo Garcia, Robert Gasca, Elie Genois, William Giang, Craig Gidney, Dar Gilboa, Raja Gosula, Alejandro Grajales Dau, Dietrich Graumann, Alex Greene, Jonathan A. Gross, Steve Habegger, John Hall, Michael C. Hamilton, Monica Hansen, Matthew P. Harrigan, Sean D. Harrington, Francisco J. H. Heras, Stephen Heslin, Paula Heu, Oscar Higgott, Gordon Hill, Jeremy Hilton, George Holland, Sabrina Hong, Hsin-Yuan Huang, Ashley Huff, William J. Huggins, Lev B. Ioffe, Sergei V. Isakov, Justin Iveland, Evan Jeffrey, Zhang Jiang, Cody Jones, Stephen Jordan, Chaitali Joshi, Pavol Juhas, Dvir Kafri, Hui Kang, Amir H. Karamlou, Kostyantyn Kechedzhi, Julian Kelly, Trupti Khaire, Tanuj Khattar, Mostafa Khezri, Seon Kim, Paul V. Klimov, Andrey R. Klots, Bryce Kobrin, Pushmeet Kohli, Alexander N. Korotkov, Fedor Kostritsa, Robin Kothari, Borislav Kozlovskii, John Mark Kriekbaum, Vladislav D. Kurilovich, Nathan Lacroix, David Landhuis, Tiano Lange-Dei, Brandon W. Langley, Pavel Laptev, Kim-Ming Lau, Loïck Le Guevel, Justin Ledford, Kenny Lee, Yuri D. Lensky, Shannon Leon, Brian J. Lester, Wing Yan Li, Yin Li, Alexander T. Lill, Wayne Liu, William P. Livingston, Aditya Locharla, Erik Lucero, Daniel Lundahl, Aaron Lunt, Sid Madhuk, Fionn D. Malone, Ashley Maloney, Salvatore Mandrà, Leigh S. Martin, Steven Martin, Orion Martin, Cameron Maxfield, Jarrod R. McClean, Matt McEwen, Seneca Meeks, Anthony Megrant, Xiao Mi, Kevin C. Miao, Amanda Mieszala, Reza Molavi, Sebastian Molina, Shirin Montazeri, Alexis Morvan, Ramis Movassagh, Wojciech Mruczkiewicz, Ofer Naaman, Matthew Neeley, Charles Neill, Ani Nersisyan, Hartmut Neven, Michael Newman, Jiun How Ng, Anthony Nguyen, Murray Nguyen, Murphy Yuezhen Niu, Thomas E. O'Brien, Alex Opremcak, John Platt, Andre Petukhov, Rebecca Potter, Leonid P. Pryadko, Chris Quintana, Pedram Roushan, Nicholas C. Rubin, Negar Saei, Daniel Sank, Kannan Sankaragomathi, Kevin J. Satzinger, Henry F. Schurkus, Christopher Schuster, Michael J. Shearn, Aaron Shorter, Vladimir Shvarts, Jindra Skrzyny, Vadim Smelyanskiy, W. Clarke Smith, George Sterling, Doug Strain, Marco Szalay, Alfredo Torres, Guifre Vidal, Benjamin Villalonga, Catherine Vollgraff Heidleweiller, Steven Waltman, Shannon X. Wang, Brayden Ware, Kate Weber, Theodore White, Kristi Wong, Bryan W. K. Woo, Cheng Xing, Z. Jamie Yao, Ping Yeh, Bicheng Ying, Juhwan Yoo, Noureldin Yosri, Grayson Young, Adam Zalcman, Yaxing Zhang, Ningfeng Zhu, and Nicholas Zobrist. 2024. Quantum error correction below the surface code threshold. <https://doi.org/10.48550/ARXIV.2408.13687>
- [2] Rajeev Acharya, Igor Aleiner, Richard Allen, Trond I. Andersen, Markus Ansmann, Frank Arute, Kunal Arya, Abraham Asfaw, Juan Atalaya, Ryan Babbush, Dave Bacon, Joseph C. Bardin, Joao Basso, Andreas Bengtsson, Sergio Boixo, Gina Bortoli, Alexandre Bourassa, Jenna Bovaird, Leon Brill, Michael Broughton, Bob B. Buckley, David A. Buell, Tim Burger, Brian Burkett, Nicholas Bushnell, Yu Chen, Zijun Chen, Ben Chiaro, Josh Cogan, Roberto Collins, Paul Conner, William Courtney, Alexander L. Crook, Ben Curtin, Dripto M. Debroy, Alexander Del Toro Barba, Sean Demura, Andrew Dunsworth, Daniel Eppens, Catherine Erickson, Lara Faoro, Edward Farhi, Reza Fatemi, Leslie Flores Burgos, Ebrahim Forati, Austin G. Fowler, Brooks Foxen, William Giang, Craig Gidney, Dar Gilboa, Marissa Giustina, Alejandro Grajales Dau, Jonathan A. Gross, Steve Habegger, Michael C. Hamilton, Matthew P. Harrigan, Sean D. Harrington, Oscar Higgott, Jeremy Hilton, Markus Hoffmann, Sabrina Hong, Trent Huang, Ashley Huff, William J. Huggins, Lev B. Ioffe, Sergei V. Isakov, Justin Iveland, Evan Jeffrey, Zhang Jiang, Cody Jones, Pavol Juhas, Dvir Kafri, Kostyantyn Kechedzhi, Julian Kelly, Tanuj Khattar, Mostafa Khezri, Mária Kieferová, Seon Kim, Alexei Kitaev, Paul V. Klimov, Andrey R. Klots, Alexander N. Korotkov, Fedor Kostritsa, John Mark Kriekbaum, David Landhuis, Pavel Laptev, Kim-Ming Lau, Lily Laws, Junho Lee, Kenny Lee, Brian J. Lester, Alexander Lill, Wayne Liu, Aditya Locharla, Erik Lucero, Fionn D. Malone, Jeffrey Marshall, Orion Martin, Jarrod R. McClean, Trevor McCourt, Matt McEwen, Anthony Megrant, Bernardo Meurer Costa, Xiao Mi, Kevin C. Miao, Masoud Mohseni, Shirin Montazeri, Alexis Morvan, Emily Mount, Wojciech Mruczkiewicz, Ofer Naaman, Matthew Neeley, Charles Neill, Ani Nersisyan, Hartmut Neven, Michael Newman, Jiun How Ng, Anthony Nguyen, Murray Nguyen, Murphy Yuezhen Niu, Thomas E. O'Brien, Alex Opremcak, John Platt, Andre Petukhov, Rebecca Potter, Leonid P. Pryadko, Chris Quintana, Pedram Roushan, Nicholas C. Rubin, Negar Saei, Daniel Sank, Kannan Sankaragomathi, Kevin J. Satzinger, Henry F. Schurkus, Christopher Schuster, Andrew W. Senior, Michael J. Shearn, Aaron Shorter, Noah Shutt, Vladimir Shvarts, Shradha Singh, Volodymyr Sivak, Jindra Skrzyny, Spencer Small, Vadim Smelyanskiy, W. Clarke Smith, Rolando D. Somma, Sofia Springer, George Sterling, Doug Strain, Jordan Suchard, Aaron Szasz, Alex Sztein, Douglas Thor, Alfredo Torres, M. Mert Torunbalci, Abeer Vaishnav, Justin Vargas, Sergey Vdovichev, Guifre Vidal, Benjamin Villalonga, Catherine Vollgraff Heidleweiller, Steven Waltman, Shannon X. Wang, Brayden Ware, Kate Weber, Theodore White, Kristi Wong, Bryan W. K. Woo, Cheng Xing, Z. Jamie Yao, Ping Yeh, Bicheng Ying, Juhwan Yoo, Noureldin Yosri, Grayson Young, Adam Zalcman, Yaxing Zhang, Ningfeng Zhu, and Nicholas Zobrist. 2024. Quantum error correction below the surface code threshold. <https://doi.org/10.48550/ARXIV.2408.13687>
- [3] Narges Alavisamani, Suhas Vittal, Ramin Ayanzadeh, Poulami Das, and Moinuddin Qureshi. 2024. Promatch: Extending the Reach of Real-Time Quantum Error Correction with Adaptive Predecoding. <https://doi.org/10.48550/ARXIV.2404.03136>
- [4] Jonathan M. Baker, Casey Duckering, David I. Schuster, and Frederic T. Chong. 2021. Virtual Logical Qubits: A Compact Architecture for Fault-Tolerant Quantum Computing. *IEEE Micro* 41, 3 (May 2021), 95–101. <https://doi.org/10.1109/mm.2021.3072789>
- [5] Ben Barber, Kenton M. Barnes, Tomasz Bialas, Okan Buğdayci, Earl T. Campbell, Neil I. Gillespie, Kausar Johar, Ram Rajan, Adam W. Richardson, Luka Skoric, Camberk Topal, Mark L. Turner, and Abbas B. Ziad. 2023. A real-time, scalable, fast and highly resource efficient decoder for a quantum computer. <https://doi.org/10.48550/ARXIV.2309.05558>
- [6] Johannes Bausch, Andrew W. Senior, Francisco J H Heras, Thomas Edlich, Alex Davies, Michael Newman, Cody Jones, Kevin Satzinger, Murphy Yuezhen Niu, Sam Blackwell, George Holland, Dvir Kafri, Juan Atalaya, Craig Gidney, Demis Hassabis, Sergio Boixo, Hartmut Neven, and Pushmeet Kohli. 2023. Learning to Decode the Surface Code with a Recurrent, Transformer-Based Neural Network. <https://doi.org/10.48550/ARXIV.2310.05900>
- [7] Michael Beverland, Vadym Kliuchnikov, and Eddie Schoute. 2022. Surface Code Compilation via Edge-Disjoint Paths. *PRX Quantum* 3, 2 (May 2022). <https://doi.org/10.1103/prxquantum.3.020342>
- [8] Michael E. Beverland, Prakash Murali, Matthias Troyer, Krysta M. Svore, Torsten Hoefler, Vadym Kliuchnikov, Guang Hao Low, Mathias Soeken, Aarthi Sundaram, and Alexander Vaschillo. 2022. Assessing requirements to scale to practical quantum advantage. <https://doi.org/10.48550/ARXIV.2211.07629>
- [9] Nick S. Blunt, György P. Gehér, and Alexandra E. Moylett. 2024. Compilation of a simple chemistry application to quantum error correction primitives. *Physical Review Research* 6, 1 (March 2024). <https://doi.org/10.1103/physrevresearch.6.013325>
- [10] Dolev Bluvstein, Simon J. Evered, Alexandra A. Geim, Sophie H. Li, Hengyun Zhou, Tom Manovitz, Sepehr Ebadi, Madelyn Cain, Marcin Kalinowski, Dominik Hangleiter, J. Pablo Bonilla Ataides, Nishad Maskara, Iris Cong, Xun Gao, Pedro Sales Rodriguez, Thomas Karolyshyn, Giulia Semeghini, Michael J. Gullans, Markus Greiner, Vladan Vuletić, and Mikhail D. Lukin. 2023. Logical quantum processor based on reconfigurable atom arrays. *Nature* 626, 7997 (Dec. 2023), 58–65. <https://doi.org/10.1038/s41586-023-06927-3>
- [11] Héctor Bombín, Chris Dawson, Ye-Hua Liu, Naomi Nickerson, Fernando Pastawski, and Sam Roberts. 2023. Modular decoding: parallelizable real-time decoding for quantum computers. <https://doi.org/10.48550/ARXIV.2303.04846>
- [12] Sergey Bravyi, Andrew W. Cross, Jay M. Gambetta, Dmitri Maslov, Patrick Rall, and Theodore J. Yoder. 2024. High-threshold and low-overhead fault-tolerant quantum memory. *Nature* 627, 8005 (March 2024), 778–782. <https://doi.org/10.1038/s41586-024-07107-7>
- [13] Sergey Bravyi and Jeongwan Haah. 2012. Magic-state distillation with low overhead. *Physical Review A* 86, 5 (Nov. 2012). <https://doi.org/10.1103/physreva.86.052329>
- [14] Keith A. Britt and Travis S. Humble. 2017. High-Performance Computing with Quantum Processing Units. *ACM Journal on Emerging Technologies in Computing Systems* 13, 3 (March 2017), 1–13. <https://doi.org/10.1145/3007651>
- [15] Ilkwon Byun, Junpyo Kim, Dongmoon Min, Ikki Nagaoka, Kosuke Fukumitsu, Iori Ishikawa, Teruo Tanimoto, Masamitsu Tanaka, Koji Inoue, and Jangwoo Kim. 2022. XQsim: modeling cross-technology control processors for 10+K qubit quantum computers. In *Proceedings of the 49th Annual International Symposium on Computer Architecture (ISCA '22)*. ACM. <https://doi.org/10.1145/3470496.3527417>
- [16] Laura Caune, Brendan Reid, Joan Camps, and Earl Campbell. 2023. Belief propagation as a partial decoder. <https://doi.org/10.48550/ARXIV.2306.17142>
- [17] Andrew Cross, Zhiyang He, Patrick Rall, and Theodore Yoder. 2024. Improved QLDPC Surgery: Logical Measurements and Bridging Codes. [arXiv:2407.18393 \[quant-ph\]](https://arxiv.org/abs/2407.18393) <https://arxiv.org/abs/2407.18393>
- [18] Andrew W. Cross, Lev S. Bishop, John A. Smolin, and Jay M. Gambetta. 2017. Open Quantum Assembly Language. <https://doi.org/10.48550/ARXIV.1707.03429>
- [19] M. P. da Silva, C. Ryan-Anderson, J. M. Bello-Rivas, A. Chernoguzov, J. M. Dreiling, C. Foltz, F. Frachon, J. P. Gaebler, T. M. Gatterman, L. Grans-Samuelsson, D. Hayes, N. Hewitt, J. Johansen, D. Lucchetti, M. Mills, S. A. Moses, B. Neyenhuis, A. Paz, J. Pino, P. Siegfried, J. Strabley, A. Sundaram, D. Tom, S. J. Wernli, M.

- Zanner, R. P. Stutz, and K. M. Svore. 2024. Demonstration of logical qubits and repeated error correction with better-than-physical error rates. <https://doi.org/10.48550/ARXIV.2404.02280>
- [20] Poulami Das, Aditya Locharla, and Cody Jones. 2022. LILLIPUT: a lightweight low-latency lookup-table decoder for near-term Quantum error correction. In *Proceedings of the 27th ACM International Conference on Architectural Support for Programming Languages and Operating Systems (ASPLOS '22)*. ACM. <https://doi.org/10.1145/3503222.3507707>
- [21] Poulami Das, Christopher A. Pattison, Srilatha Manne, Douglas M. Carmean, Krysta M. Svore, Moinuddin Qureshi, and Nicolas Delfosse. 2022. AFS: Accurate, Fast, and Scalable Error-Decoding for Fault-Tolerant Quantum Computers. In *2022 IEEE International Symposium on High-Performance Computer Architecture (HPCA)*. IEEE. <https://doi.org/10.1109/hpca53966.2022.00027>
- [22] Nicolas Delfosse. 2020. Hierarchical decoding to reduce hardware requirements for quantum computing. <https://doi.org/10.48550/ARXIV.2001.11427>
- [23] Nicolas Delfosse, Andres Paz, Alexander Vaschillo, and Krysta M. Svore. 2023. How to choose a decoder for a fault-tolerant quantum computer? The speed vs accuracy trade-off. <https://doi.org/10.48550/ARXIV.2310.15313>
- [24] Yongshan Ding, Adam Holmes, Ali Javadi-Abhari, Diana Franklin, Margaret Martonosi, and Frederic Chong. 2018. Magic-State Functional Units: Mapping and Scheduling Multi-Level Distillation Circuits for Fault-Tolerant Quantum Architectures. In *2018 51st Annual IEEE/ACM International Symposium on Microarchitecture (MICRO)*. IEEE. <https://doi.org/10.1109/micro.2018.00072>
- [25] Austin G. Fowler. 2015. Minimum weight perfect matching of fault-tolerant topological quantum error correction in average $O(1)$ parallel time. *Quantum Info. Comput.* 15, 1–2 (jan 2015), 145–158.
- [26] Austin G. Fowler, Matteo Mariantoni, John M. Martinis, and Andrew N. Cleland. 2012. Surface codes: Towards practical large-scale quantum computation. *Physical Review A* 86, 3 (Sept. 2012). <https://doi.org/10.1103/physreva.86.032324>
- [27] Spiro Gicev, Lloyd C. L. Hollenberg, and Muhammad Usman. 2023. A scalable and fast artificial neural network syndrome decoder for surface codes. *Quantum* 7 (July 2023), 1058. <https://doi.org/10.22331/q-2023-07-12-1058>
- [28] Craig Gidney. 2021. Stim: a fast stabilizer circuit simulator. *Quantum* 5 (July 2021), 497. <https://doi.org/10.22331/q-2021-07-06-497>
- [29] Anqi Gong, Sebastian Cammerer, and Joseph M. Renes. 2024. Toward Low-latency Iterative Decoding of QLDPC Codes Under Circuit-Level Noise. <https://doi.org/10.48550/ARXIV.2403.18901>
- [30] Riddhi S. Gupta, Neeraja Sundaresan, Thomas Alexander, Christopher J. Wood, Seth T. Merkel, Michael B. Healy, Marius Hillenbrand, Tomas Joehym-O'Connor, James R. Wootton, Theodore J. Yoder, Andrew W. Cross, Maika Takita, and Benjamin J. Brown. 2024. Encoding a magic state with beyond break-even fidelity. *Nature* 625, 7994 (Jan. 2024), 259–263. <https://doi.org/10.1038/s41586-023-06846-3>
- [31] Oscar Higgott and Craig Gidney. 2023. Sparse Blossom: correcting a million errors per core second with minimum-weight matching. <https://doi.org/10.48550/ARXIV.2303.15933>
- [32] Timo Hillmann, Lucas Berent, Armanda O. Quintavalle, Jens Eisert, Robert Wille, and Joschka Roffe. 2024. Localized statistics decoding: A parallel decoding algorithm for quantum low-density parity-check codes. <https://doi.org/10.48550/ARXIV.2406.18655>
- [33] Dominic Horsman, Austin G Fowler, Simon Devitt, and Rodney Van Meter. 2012. Surface code quantum computing by lattice surgery. *New Journal of Physics* 14, 12 (Dec. 2012), 123011. <https://doi.org/10.1088/1367-2630/14/12/123011>
- [34] Junpyo Kim, Dongmoon Min, Jungmin Cho, Hyeonseong Jeong, Ilkwon Byun, Junhyuk Choi, Juwon Hong, and Jangwoo Kin. 2024. A Fault-Tolerant Million Qubit-Scale Distributed Quantum Computer. In *Proceedings of the 27th ACM International Conference on Architectural Support for Programming Languages and Operating Systems*. ACM. <https://doi.org/10.1145/3620665.3640388>
- [35] Emanuel Knill and Raymond Laflamme. 1997. Theory of quantum error-correcting codes. *Physical Review A* 55, 2 (Feb. 1997), 900–911. <https://doi.org/10.1103/physreva.55.900>
- [36] Tyler Leblond, Christopher Dean, George Watkins, and Ryan Bennink. 2024. Realistic Cost to Execute Practical Quantum Circuits using Direct Clifford+T Lattice Surgery Compilation. *ACM Transactions on Quantum Computing* 5, 4 (Oct. 2024), 1–28. <https://doi.org/10.1145/3689826>
- [37] Ang Li, Samuel Stein, Sriram Krishnamoorthy, and James Ang. 2023. QASMBench: A Low-Level Quantum Benchmark Suite for NISQ Evaluation and Simulation. *ACM Transactions on Quantum Computing* 4, 2 (Feb. 2023), 1–26. <https://doi.org/10.1145/3550488>
- [38] Sophia Fuhui Lin, Joshua Viszlai, Kaitlin N. Smith, Gokul Subramanian Ravi, Charles Yuan, Frederic T. Chong, and Benjamin J. Brown. 2023. Codesign of quantum error-correcting codes and modular chiplets in the presence of defects. <https://doi.org/10.48550/ARXIV.2305.00138>
- [39] Daniel Litinski. 2019. A Game of Surface Codes: Large-Scale Quantum Computing with Lattice Surgery. *Quantum* 3 (March 2019), 128. <https://doi.org/10.22331/q-2019-03-05-128>
- [40] Daniel Litinski. 2019. Magic State Distillation: Not as Costly as You Think. *Quantum* 3 (Dec. 2019), 205. <https://doi.org/10.22331/q-2019-12-02-205>
- [41] C. L. Liu and James W. Layland. 1973. Scheduling Algorithms for Multiprogramming in a Hard-Real-Time Environment. *J. ACM* 20, 1 (Jan. 1973), 46–61. <https://doi.org/10.1145/321738.321743>
- [42] Matt McEwen, Lara Faoro, Kunal Arya, Andrew Dunsworth, Trent Huang, Seon Kim, Brian Burkett, Austin Fowler, Frank Arute, Joseph C. Bardin, Andreas Bengtsson, Alexander Bilmes, Bob B. Buckley, Nicholas Bushnell, Zijun Chen, Roberto Collins, Sean Demura, Alan R. Derk, Catherine Erickson, Marissa Giustina, Sean D. Harrington, Sabrina Hong, Evan Jeffrey, Julian Kelly, Paul V. Klimov, Fedor Kostritsa, Pavel Laptev, Aditya Locharla, Xiao Mi, Kevin C. Miao, Shirin Montazeri, Josh Mutus, Ofer Naaman, Matthew Neeley, Charles Neill, Alex Opremcak, Chris Quintana, Nicholas Redd, Pedram Roushan, Daniel Sank, Kevin J. Satzinger, Vladimir Shvarts, Theodore White, Z. Jamie Yao, Ping Yeh, Juhwan Yoo, Yu Chen, Vadim Smelyanskiy, John M. Martinis, Hartmut Neven, Anthony Megrant, Lev Ioffe, and Rami Barends. 2021. Resolving catastrophic error bursts from cosmic rays in large arrays of superconducting qubits. *Nature Physics* 18, 1 (Dec. 2021), 107–111. <https://doi.org/10.1038/s41567-021-01432-8>
- [43] Kai Meinerz, Chae-Yeun Park, and Simon Trebst. 2022. Scalable Neural Decoder for Topological Surface Codes. *Physical Review Letters* 128, 8 (Feb. 2022). <https://doi.org/10.1103/physrevlett.128.080505>
- [44] Kevin C. Miao, Matt McEwen, Juan Atalaya, Dvir Kafri, Leonid P. Pryadko, Andreas Bengtsson, Alex Opremcak, Kevin J. Satzinger, Zijun Chen, Paul V. Klimov, Chris Quintana, Rajeev Acharya, Kyle Anderson, Markus Ansmann, Frank Arute, Kunal Arya, Abraham Asfaw, Joseph C. Bardin, Alexandre Bourassa, Jenna Bovard, Leon Brill, Bob B. Buckley, David A. Buell, Tim Burger, Brian Burkett, Nicholas Bushnell, Juan Campero, Ben Chiaro, Roberto Collins, Paul Conner, Alexander L. Crook, Ben Curtin, Dripto M. Debroy, Sean Demura, Andrew Dunsworth, Catherine Erickson, Reza Fatemi, Vinicius S. Ferreira, Leslie Flores Burgos, Ebrahim Forati, Austin G. Fowler, Brooks Foxen, Gonzalo Garcia, William Giang, Craig Gidney, Marissa Giustina, Raja Gosula, Alejandro Grajales Dau, Jonathan A. Gross, Michael C. Hamilton, Sean D. Harrington, Paula Heu, Jeremy Hilton, Markus R. Hoffmann, Sabrina Hong, Trent Huang, Ashley Huff, Justin Iveland, Evan Jeffrey, Zhang Jiang, Cody Jones, Julian Kelly, Seon Kim, Fedor Kostritsa, John Mark Kreikebaum, David Landhuis, Pavel Laptev, Lily Laws, Kenny Lee, Brian J. Lester, Alexander T. Lill, Wayne Liu, Aditya Locharla, Erik Lucero, Steven Martin, Anthony Megrant, Xiao Mi, Shirin Montazeri, Alexis Morvan, Ofer Naaman, Matthew Neeley, Charles Neill, Ani Nersisyan, Michael Newman, Jiun How Ng, Anthony Nguyen, Murray Nguyen, Rebecca Potter, Charles Roque, Pedram Roushan, Kannan Sankaragomathi, Henry F. Schurkus, Christopher Schuster, Michael J. Shearn, Aaron Shorter, Noah Shutty, Vladimir Shvarts, Jindra Skrzuzny, W. Clarke Smith, George Sterling, Marco Szalay, Douglas Thor, Alfredo Torres, Theodore White, Bryan W. K. Woo, Z. Jamie Yao, Ping Yeh, Juhwan Yoo, Grayson Young, Adam Zalcman, Ningfeng Zhu, Nicholas Zobrist, Hartmut Neven, Vadim Smelyanskiy, Andre Petukhov, Alexander N. Korotkov, Daniel Sank, and Yu Chen. 2023. Overcoming leakage in quantum error correction. *Nature Physics* 19, 12 (Oct. 2023), 1780–1786. <https://doi.org/10.1038/s41567-023-02226-w>
- [45] Ramon W. J. Overwater, Masoud Babaie, and Fabio Sebastiani. 2022. Neural-Network Decoders for Quantum Error Correction Using Surface Codes: A Space Exploration of the Hardware Cost-Performance Tradeoffs. *IEEE Transactions on Quantum Engineering* 3 (2022), 1–19. <https://doi.org/10.1109/tqe.2022.3174017>
- [46] Nils Quetschlich, Lukas Burgholzer, and Robert Wille. 2023. MQT Bench: Benchmarking Software and Design Automation Tools for Quantum Computing. *Quantum* (2023). MQT Bench is available at <https://www.cda.cit.tum.de/mqtbench/>
- [47] Gokul Subramanian Ravi, Jonathan M. Baker, Arash Fayyazi, Sophia Fuhui Lin, Ali Javadi-Abhari, Massoud Pedram, and Frederic T. Chong. 2023. Better Than Worst-Case Decoding for Quantum Error Correction. In *Proceedings of the 28th ACM International Conference on Architectural Support for Programming Languages and Operating Systems, Volume 2 (ASPLOS '23)*. ACM. <https://doi.org/10.1145/3575693.3575733>
- [48] Joschka Roffe, David R. White, Simon Burton, and Earl Campbell. 2020. Decoding across the quantum low-density parity-check code landscape. *Physical Review Research* 2, 4 (Dec. 2020). <https://doi.org/10.1103/physrevresearch.2.043423>
- [49] Neil J. Ross and Peter Selinger. 2014. Optimal ancilla-free Clifford+T approximation of z-rotations. <https://doi.org/10.48550/ARXIV.1403.2975>
- [50] Peter W. Shor. 1995. Scheme for reducing decoherence in quantum computer memory. *Physical Review A* 52, 4 (Oct. 1995), R2493–R2496. <https://doi.org/10.1103/physreva.52.r2493>
- [51] Luka Skoric, Dan E. Browne, Kenton M. Barnes, Neil I. Gillespie, and Earl T. Campbell. 2023. Parallel window decoding enables scalable fault tolerant quantum computation. *Nature Communications* 14, 1 (Nov. 2023). <https://doi.org/10.1038/s41467-023-42482-1>
- [52] Samuel C. Smith, Benjamin J. Brown, and Stephen D. Bartlett. 2023. Local Predecoder to Reduce the Bandwidth and Latency of Quantum Error Correction. *Physical Review Applied* 19, 3 (March 2023). <https://doi.org/10.1103/physrevapplied.19.034050>
- [53] Samuel Stein, Sara Sussman, Teague Tomesh, Charles Guinn, Esin Tureci, Sophia Fuhui Lin, Wei Tang, James Ang, Srivatsan Chakram, Ang Li, Margaret

- Martonosi, Fred Chong, Andrew A. Houck, Isaac L. Chuang, and Michael Demarco. 2023. HetArch: Heterogeneous Microarchitectures for Superconducting Quantum Systems. In *56th Annual IEEE/ACM International Symposium on Microarchitecture (MICRO '23)*. ACM. <https://doi.org/10.1145/3613424.3614300>
- [54] Samuel Stein, Shifan Xu, Andrew W. Cross, Theodore J. Yoder, Ali Javadi-Abhari, Chenxu Liu, Kun Liu, Zeyuan Zhou, Charles Guinn, Yufei Ding, Yongshan Ding, and Ang Li. 2024. Architectures for Heterogeneous Quantum Error Correction Codes. <https://doi.org/10.48550/ARXIV.2411.03202>
- [55] Yasunari Suzuki, Takanori Sugiyama, Tomochika Arai, Wang Liao, Koji Inoue, and Teruo Tanimoto. 2022. Q3DE: A fault-tolerant quantum computer architecture for multi-bit burst errors by cosmic rays. In *2022 55th IEEE/ACM International Symposium on Microarchitecture (MICRO)*. IEEE, 1110–1125. <https://doi.org/10.1109/micro56248.2022.00079>
- [56] Xinyu Tan, Fang Zhang, Rui Chao, Yaoyun Shi, and Jianxin Chen. 2022. Scalable surface code decoders with parallelization in time. <https://doi.org/10.48550/ARXIV.2209.09219>
- [57] Barbara M. Terhal. 2015. Quantum error correction for quantum memories. *Reviews of Modern Physics* 87, 2 (April 2015), 307–346. <https://doi.org/10.1103/revmodphys.87.307>
- [58] Yu Tomita and Krysta M. Svore. 2014. Low-distance surface codes under realistic quantum noise. *Physical Review A* 90, 6 (Dec. 2014). <https://doi.org/10.1103/physreva.90.062320>
- [59] Yosuke Ueno, Masaaki Kondo, Masamitsu Tanaka, Yasunari Suzuki, and Yutaka Tabuchi. 2021. QECool: On-Line Quantum Error Correction with a Superconducting Decoder for Surface Code. In *2021 58th ACM/IEEE Design Automation Conference (DAC)*. IEEE. <https://doi.org/10.1109/dac18074.2021.9586326>
- [60] Yosuke Ueno, Masaaki Kondo, Masamitsu Tanaka, Yasunari Suzuki, and Yutaka Tabuchi. 2022. NEO-QEC: Neural Network Enhanced Online Superconducting Decoder for Surface Codes. <https://doi.org/10.48550/ARXIV.2208.05758>
- [61] Savvas Varsamopoulos, Ben Criger, and Koen Bertels. 2017. Decoding small surface codes with feedforward neural networks. *Quantum Science and Technology* 3, 1 (Nov. 2017), 015004. <https://doi.org/10.1088/2058-9565/aa955a>
- [62] Suhas Vittal, Poulami Das, and Moinuddin Qureshi. 2023. Astrea: Accurate Quantum Error-Decoding via Practical Minimum-Weight Perfect-Matching. In *Proceedings of the 50th Annual International Symposium on Computer Architecture (ISCA '23)*. ACM. <https://doi.org/10.1145/3579371.3589037>
- [63] George Watkins, Hoang Minh Nguyen, Keelan Watkins, Steven Pearce, Hoi-Kwan Lau, and Alexandru Paler. 2024. A High Performance Compiler for Very Large Scale Surface Code Computations. *Quantum* 8 (May 2024), 1354. <https://doi.org/10.22331/q-2024-05-22-1354>
- [64] Stasiu Wolanski and Ben Barber. 2024. Ambiguity Clustering: an accurate and efficient decoder for qLDPC codes. <https://doi.org/10.48550/ARXIV.2406.14527>
- [65] Yue Wu, Namitha Liyanage, and Lin Zhong. 2022. An interpretation of Union-Find Decoder on Weighted Graphs. <https://doi.org/10.48550/ARXIV.2211.03288>
- [66] Abbas B. Ziad, Ankit Zalawadiya, Canberk Topal, Joan Camps, György P. Gehér, Matthew P. Stafford, and Mark L. Turner. 2024. Local Clustering Decoder: a fast and adaptive hardware decoder for the surface code. <https://doi.org/10.48550/ARXIV.2411.10343>